

MECHANICAL AND VACUUM STABILITY DESIGN CRITERIA FOR THE LHC EXPERIMENTAL VACUUM CHAMBERS

I.R. Collins, O. Gröbner, P. Lepeule, R. Veness, CERN, Geneva, Switzerland

Abstract

Four colliding beam experiments are planned for the Large Hadron Collider (LHC) requiring experimental vacuum chambers in the interaction region. The beam pipe should be as transparent as possible to scattered particles and detectors should be as close as possible to the interaction point, resulting in small diameter beam pipes. This, together with the bunched beam structure, makes ion induced pressure bump instability, well-known from the Intersecting Storage Rings (ISR) at CERN, a potential problem. Adequate conductance, cleanliness of the beam pipes and efficient pumping are required to avoid this instability. Suppression of electron multipacting requires appropriate surface coatings and cleaning procedures. Small beam pipe diameters must provide the required beam stay clear and still allow margin for alignment and stability inside detectors. Design criteria to ensure both local and global stability under static and dynamic mechanical loads are defined.

1 INTRODUCTION

All four experiments, ATLAS, CMS, LHCb and ALICE have different requirements, not only for static vacuum but also for beam pipe diameters and materials as well as space dedicated to vacuum equipment. Nevertheless, since all experiments share the same beams, a common, safe set of design criteria must be established which includes dynamic vacuum stability for the ultimate beam intensity (0.85A) and the mechanical design of the beam pipe. In this way, both the correct operation of the machine and the mechanical integrity of the beam pipe can be ensured.

2 ION INDUCED PRESSURE INSTABILITY

Ion induced pressure runaway was a serious limitation of the proton beam intensity stored in the ISR. This pressure instability may occur when positive ions, created by ionisation of the residual gas and repelled by the space charge of the beam, bombard the vacuum chamber wall and desorb tightly bound molecules. Since desorbed gas may in turn be ionised, this feedback mechanism can result in a pressure runaway. The pressure increases with beam current from the initial value, P_o , as

$$P_I = \frac{P_o}{1 - \frac{\eta I}{(\eta I)_{crit}}}$$
 and will double at half the value of $(\eta I)_{crit}$. The pressure remains stable as long as the beam

current is below a critical value given by $I_c = \frac{e}{\eta \sigma} S_{eff}$

where e is the charge of the electron, η the net ion desorption yield (molecules per ion), σ the ionisation cross section of the residual gas molecules for high energy protons and S_{eff} represents a linear, effective pumping speed. The required static pressure to achieve negligible background from beam-gas scattering can be obtained in most cases without difficulty. To guarantee vacuum stability, however, a clean vacuum chamber with a low η for all residual gas components and a sufficiently large effective pumping speed must be provided. The ionisation cross sections for relativistic protons (7 TeV) can be calculated [1] and are of the order of 0.4 to 2.8 10^{-22} m² for H₂ and CO₂ respectively. The effective, linear pumping speed depends on the design of the vacuum system and in most practical situations, is limited by the conductance of the beam pipe and the location of pumps. The vacuum stability for the arcs of LHC and for the experiments has been studied extensively [2, 3].

2.1 Ion induced molecular desorption yields

Molecular desorption yields obtained in laboratory measurements and derived from observations with beam in the ISR can be found in [4]. Incident ion energy and surface cleanliness are important for the desorption rate. Vacuum conditioning which had been applied successfully in the ISR machine includes *in-situ* bakeout at 300°C for 24 hours and argon ion glow discharge (ArGDC) cleaning followed again by *in-situ* bakeout. The net yield in a machine, where ions are produced from the residual gas and the corresponding yields measured in the laboratory using an external ion source are related by $\eta_{machine} = \eta_{lab} - 1$. Typical molecular desorption yields which may be used for the vacuum design are given in Table 1. These data have been derived from laboratory measurements but experience in the ISR has shown that measurements on small samples may give results which are not representative for a real machine. Values for η which are considered to be more realistic and their dependence on ion energy are shown in Figure 1. For energies above 3 keV the yield saturates and these saturated values have been chosen to calculate the vacuum stability for the experiments. To calculate the critical current for a practical system, a ‘safety factor’ of at least 2 must be applied to account for the inherent uncertainty of the desorption data, the fact that in a gas mixture one species may desorb others and finally to account for the doubling of the pressure which will occur at half the critical current.

Table 1. Molecular desorption yield (η_{lab}) for 1.4 keV K^+ ions for unbaked, 24 hours at 300°C *in-situ* baked and for argon ion glow discharge cleaned and again *in-situ* baked stainless steel (ArGDC) with 2 keV N_2 ions [5,6].

Gas	Molecular desorption yield η_{lab} (in molecules ion ⁻¹)		
	unbaked	300°C baked <i>in-situ</i>	ArGDC, and baked
H ₂	9	4	0.5
CH ₄	0.5	0.2	<0.1
CO	7	3	1
CO ₂	2	0.5	<0.01

2.2 Ion impact energy

Ions created from the residual gas are accelerated away from the beam due to the kicks of successive bunches. Light ions experience more strongly the peak electric field and thus gain more energy than heavier ions. In the regular arc of LHC, the ion impact energy for CO is close to 300 eV.

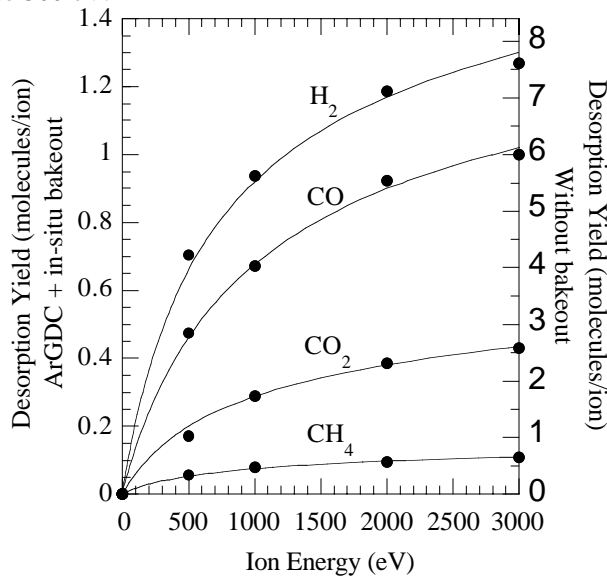


Figure 1. Dependence of the desorption yield on ion energy for unbaked and baked stainless steel after ArGDC.

The ion impact energy as a function of the distance from a high luminosity intersection (ATLAS, CMS) and 0.85 A is shown in Figure 2. The effect of an external magnetic field has not been taken into account.

3 ELECTRON MULTIPACTING

The build-up of a cloud of secondary electrons due to the interaction with the bunched proton beam is a potential problem in the LHC since the bombardment of the vacuum chamber wall by energetic electrons (several hundred eV) could produce gas desorption and excessive pressure rise [7]. A critical parameter for this effect is the

secondary electron yield for which a safe value ($\delta_{max} \leq 1.4$) will be provided by a suitable surface coating and by bakeout of the beam pipe [8].

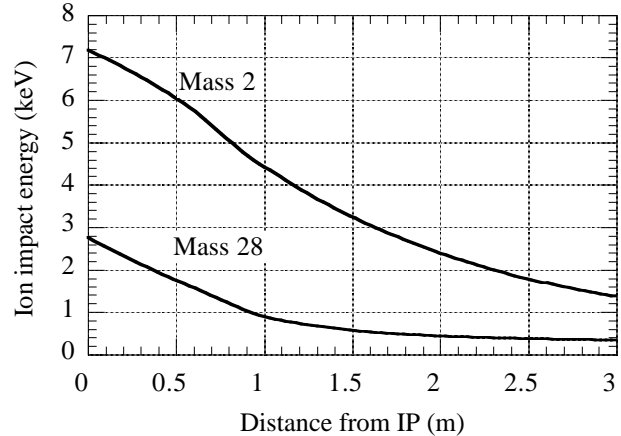


Figure 2. Ion impact energy near a high luminosity IP

4 MECHANICAL APERTURE

The beam pipe must stay clear from the beam halo to avoid particle loss and background. Inside the massive detectors, beam pipes must be supported at a height of up to 11.5m from the ground while the newly constructed caverns may be subject to settling movements. The adopted scheme is to align beam pipes to a theoretical axis before final closing of the experiments, and to adjust the position of the detectors between running periods. No active monitoring or alignment of the beam pipe is foreseen due to difficulties in accessing reference points from outside the closed experiment. Four elements are required to define the mechanical beam pipe aperture: beam size (9.8 beam σ at injection including closed orbit variations); beam pipe manufacturing tolerances; precision with which fiducial survey marks can be referred to the theoretical beam axis and the precision to which detectors can be kept aligned to this axis. These four elements differ between the experiments, but impose a minimum vacuum chamber diameter between 40 and 60 mm.

5 MECHANICAL STABILITY

Experimental beam pipes operate under 1 bar of external pressure. They support a small distributed load due to their weight and bakeout equipment. The failure mode is therefore by elastic instability, leading to collapse (buckling) rather than yielding. The basic model assumes a long cylindrical thin-walled shell with perfect initial geometry. For a buckling mode of 2, the critical pressure P_{cr} at which the tube collapses depends on the radius r , wall thickness t , elastic modulus E , and Poisson's ratio ν [9].

$$P_{cr} = \frac{1}{4} \frac{E}{(1-\nu^2)} \frac{t^3}{r^3}.$$

The adopted design criterion requires $P_{Cr} \geq 4$ bar for simple machined shapes and $P_{Cr} \geq 6$ for complex and fabricated structures (beryllium pipes). The second design criterion requires supports to be placed such that the resulting bending deflections are smaller than the wall thickness. These safety margins are necessary since P_{Cr} is sensitive to form imperfections (particularly in welded and fabricated chambers) and to ovalisation by axial bending moments. In critical areas of the experiments, and for complex geometries, such simple criteria will not provide a well optimised structure. Here a full non-linear finite element analysis of the beam pipe including supports is required. The analysis must include estimations of initial imperfections, based on the proposed manufacturing techniques and the influence of longitudinal bending moments on P_{Cr} (Brazier effect). After this analysis, design values of P_{Cr} can be safely reduced to 3 bar [10]. Vacuum chamber elements have little lateral stiffness and are thus prone to column buckling under compression. Compressive forces may arise from the chamber geometry and reaction forces of bellows. A safety factor of 4 is applied to the buckling pressure to allow for uncertainties in supports. This criterion determines the number of lateral supports required.

6 DYNAMICAL LOADING

Dynamic mechanical loads occur when an elastic structure vibrates under a periodic impulse. As the impulse frequency approaches the natural vibration, oscillations with large amplitude may be induced leading to fatigue and premature failure. The experimental beam pipes will consist of individual, 5 to 7m long thin walled cylinders, between 40 to 300mm diameter and linked together by bellows expansion joints. Each element is supported individually from the surrounding detector either directly, or by tensioned wires. The fundamental frequency f_n of such a simply supported tube under its own weight

w per unit length [11] is approx. $f_n = \frac{5}{\pi} \sqrt{\frac{EIg}{wl}}$, where

E is the elastic modulus, I the second moment of area, g the acceleration by gravity and l the distance between supports. Potential sources of impulses are mechanical vacuum pumps and detectors via the supports. Measurements from pumping stations have shown impulse frequencies of 50 Hz and its harmonics. Thus, to avoid resonance beam pipes will be designed for fundamental frequencies above 100 Hz. These estimates, confirmed by finite element analysis, have demonstrated the need of additional supports to those initially foreseen [12].

7 CONCLUSIONS

The critical current product and the maximum single beam current at which the most critical gas (CO) remains stable, are summarised in Table 2 based on the present layout of experiments. The assumed pumping system uses a combination of distributed getter pumps and lumped ion pumps so that inert gases (methane) are efficiently pumped.

Table 2. Critical current product for CO and maximum stable beam currents for LHC experiments

	ηI (CO)	I_{\max} (A) unbaked	I_{\max} (A) baked & ArGDC
ATLAS	4.3	0.18	1.1
CMS	4.1	0.17	1.0
LHCb	2.9	0.12	0.73
ALICE	5.2	0.22	1.3

Inspection of I_{\max} in columns 3 and 4 shows that ArGDC and *in-situ* bakeout are necessary to meet the specified beam current (ultimate current 0.85 A) with a required safety factor of 2. *In-situ* bakeout also provides safe conditions against the electron avalanche effect.

A global safety factor of 4 is required for mechanical stability against buckling but requires that lateral supports will be placed such that dynamical loading can be controlled. This factor can be reduced to 3 when a detailed analysis of the whole environment is carried out.

8 REFERENCES

- [1] F. Rieke, W. Prepejchal, PRA 6 (1972) 1507
- [2] O. Gröbner, Vacuum, No. 8, 1995, 797
- [3] W.C. Turner, J. Vac. Sci. Technol. A 14(4) (1996) 2026
- [4] E. Fischer, CERN-ISR-VA/EF/sm (1975)
- [5] A.G. Mathewson, CERN-ISR-VA/76-5 (1976)
- [6] A.G. Mathewson, Vuoto, Vol.XVII, No.3, 102, July/September, 1987.
- [7] O. Gröbner, 10th Int. Conf. on High Energy Accel., Protvino, July (1977)
- [8] I. Bojko, J-L. Dorier, N. Hilleret, Ch. Scheuerlein, CERN-LHC-VAC/Ch.S, Vacuum Technical Note 97-19, June 1997
- [9] S. Timoshenko, J. Gere, Theory of Elastic Stability, 2nd ed. Mc. Graw-Hill, 1963
- [10] A. Lugan, B. Skoczen, T. Kurtyka, CERN-EST-ESI Technical Note 97-04, June 1997
- [11] W. Young, Roark's Formulas for Stress and Strain, 6th ed. Mc. Graw-Hill, 1989
- [12] S. Mayer, B. Skoczen, CERN-EST-ESI Technical Note, November 1997